

# Enhancing noise-induced switching times in systems with distributed delays

Y.N. Kyrychko\*

*Department of Mathematics, University of Sussex,  
Falmer, Brighton, BN1 9QH, United Kingdom*

I.B. Schwartz

*US Naval Research Laboratory, Code 6792,  
Nonlinear System Dynamics Section,  
Plasma Physics Division, Washington, DC 20375, USA*

(Dated: today)

## Abstract

The paper addresses the problem of calculating the noise-induced switching rates in systems with delay-distributed kernels and Gaussian noise. A general variational formulation for the switching rate is derived for any distribution kernel, and the obtained equations of motion and boundary conditions represent the most probable, or optimal, path, which maximizes the probability of escape. Explicit analytical results for the switching rates for small mean time delays are obtained for the uniform and bi-modal (or two-peak) distributions. They suggest that increasing the width of the distribution leads to an increase in the switching times even for longer values of mean time delays for both examples of the distribution kernel, and the increase is higher in the case of the two-peak distribution. Analytical predictions are compared to the direct numerical simulations, and show excellent agreement between theory and numerical experiment.

---

\* y.kyrychko@sussex.ac.uk

Many real world dynamical systems exhibit complex behavior often induced by intrinsic time delays. In addition, the majority of such systems are influenced by both external and internal random perturbations. An important practical problem, therefore, is to understand how random disturbances are organized such that the dynamics escape from a stable attractor and exhibit new behavior. Although the noise amplitudes are small, the resulting change is a large fluctuation out of the basin of attraction. In this paper, we study the influence of noise-induced large fluctuations on dynamical systems, where the time delay is not taken as a constant but is rather chosen from a given distribution. We use a variational approach to calculate the switching rates out of the basin of attraction of the stable equilibrium for a general kernel of the delay distribution, as well as general nonlinearity. Taking two particular commonly-used examples of the distribution kernel, namely, the uniform and bi-modal kernels, we analyze how the width of the distribution affects the switching rates. Our results suggest that the switching is affected not only by the mean time delay, but also by the width of the delay distribution. Specifically, if the distribution width is increased, this leads to an increase in the switching times.

## I. INTRODUCTION

Time-delayed models have been extensively applied in various disciplines, including neuroscience, quantum optics, laser dynamics, mechanical and chemical oscillators, population dynamics, mathematical epidemiology, and many others [1]. In these systems, time delays are often used to account for a finite propagation time, the time it takes for a signal to be processed and fed back, and significant time delays can arise due to the separation between the subsystems. In neural systems, delays represent the time it takes for neural signals to propagate and be processed [2, 3], and in semiconductor lasers the delay is determined by the propagation path, and is much longer than the internal oscillation periods [4]. In quantum networks, in order to model non-Markovian aspects of quantum dynamics, one has to account for delayed interactions between network nodes when exchanging photons, and time-delayed feedback control can be used to create and stabilize entangled states [5, 6]. In order to describe population fluctuations in ecological setting, it is important to include

maturation time, the time it takes to develop into a reproducing adult [7–9]. In epidemiology, time delays can represent latency or temporary immunity periods affecting the spread of the infection [9–11], and in gene regulatory networks they arise during the transcription and translation of mRNA [12–14]. Finally, robotic systems such as swarms and their control have attracting states that only can be captured with delayed communication and control actuation [15, 16].

In addition to intrinsic time delays, majority of real systems are also affected by both external and internal random perturbations, which necessitate the inclusion of noise into the dynamical models, and hence, stochastic differential delay equations (DDEs) are used to analyze a wide range of systems. For instance, gene regulatory networks are often modeled as stochastic birth-death processes with time delays [12], and anomalies during El Niño have been analyzed using delayed-oscillator models, excited by external weather noise [17–19]. Recently, time-delayed feedback control has been applied to noise-induced chimera states in FitzHugh-Nagumo networks with non-local coupling, and it has been shown that for some values of time delays, it can lead to the so-called period-two coherence resonance chimera [20]. Much of the analysis of stochastic DDEs involving local fluctuations has been done using delayed Fokker-Plank equations, and several small delay approximation methods have been suggested. Furthermore, a perturbation theory method has been developed to determine single time point probability densities and mean delays, as well as autocorrelation functions in stochastic SDEs in the context of delayed Fokker-Plank equations [21, 22].

In this paper we focus on understanding large fluctuations in dynamical systems with distributed time delays, which have one or more stable steady states. In the absence of noise, the solutions will go to a stable steady state; however, when the noise is included, even if small in intensity, it leads to fluctuations around the stable steady state. Furthermore, noise can force the system out of the stable steady state, or it can lead to switching to another stable steady state. This phenomenon is similar to the tipping process in dynamical systems, where relatively small changes in input can lead to sudden and disproportional changes in output, for example, due to a slow variation in parameter (B-tipping) or inclusion of noise (N-tipping) [23–25]. For systems not in thermal equilibrium, as in the case of noise-induced switching between states, the probability distribution is no longer of the Boltzmann form. Many results have been obtained for dynamical systems without delay driven by white Gaussian noise and for Markovian reaction and population systems, cf. [26–37].

On the other hand, noise-induced switching has been studied for bistable systems in the presence of time delay to demonstrate residence times depending on the noise level, as well as to analytically calculate the expressions for the autocorrelation function and power spectrum [38, 39]. Switching entire behaviors for complex discrete delay-coupled swarming systems has been observed in [40]. Noise-induced switching rates between stable steady states, and the rates of noise-induced extinction in the case of constant time delays, have recently been analyzed in general in [41]. In this paper we will study a time-delayed system driven by noise, where the time delay is given by an integral with a memory kernel in the form of the prescribed delay distribution function. The research in this paper is motivated by the effects of distributed delays on the system dynamics in various settings; for example, in models coupled oscillators [42–44], in traffic dynamics to describe the memory effects on drivers [45], to represent long-range interactions between neurons [3, 46], modeling waiting times in epidemiological models [47], as well as maturation periods in population dynamics modeling [48, 49].

The outline of the paper is as follows. In Section II we apply variational approach to formulate the problem in order to calculate the rate of switching out of the basin of attraction of the steady state for a general delay distribution and general nonlinearity. In Section III, we consider the case of the uniformly distributed delay kernel, and show how the width of the distribution influences the switching rate. The case of the two-peak delay distribution is analyzed in Section IV, and the results are compared to the case of the uniform distribution. For both types of distributions, we perform numerical simulations, which are presented in Section V, and the agreement between theory and analytical results is excellent.

## II. GENERAL CASE OF THE DELAY DISTRIBUTION KERNEL

We consider a switching process in a one-dimensional system with distributed time delay and noise, which has the form

$$\dot{x}(t) = f\left(x(t), \int_0^\infty g(\sigma)x(t-\sigma)d\sigma\right) + \eta(t), \quad (1)$$

where the distribution kernel  $g(\cdot)$  is assumed to be non-negative and normalized to unity, i.e.

$$g(s) \geq 0, \quad \int_0^\infty g(s)ds = 1,$$

$\eta(t)$  is the noise, and  $f(\cdot)$  is a nonlinear function. If  $g(u) = \delta(u)$ , one obtains a system without time delays, and if  $g(u) = \delta(u - \tau)$ , this leads to the case of discrete time delay.

In the case of Gaussian noise, if  $D$  is the noise intensity, one can characterize noise realizations  $\eta(t)$  by its probability density functional  $\mathcal{P}_\eta[\eta(t)] \approx \exp(-\mathcal{R}_\eta/D)$  with

$$\mathcal{R}_\eta[\eta(t)] = \frac{1}{4} \int_{-\infty}^{\infty} dt dt' \eta(t) \hat{\mathcal{F}}(t - t') \eta(t'), \quad (2)$$

where  $\hat{\mathcal{F}}(t - t')/2D$  is the inverse of the pair correlator of  $\eta(t)$  [50]. Noise intensity  $D$  is assumed to be sufficiently small, so that sample paths will limit on an optimal path as  $D \rightarrow 0$ .

In the absence of noise, we consider a situation in which the system possesses a stable steady state,  $x_A$ , and a saddle point,  $x_S$ , satisfying  $f(x_A, x_A) = f(x_S, x_S) \equiv 0$ . For the topological switching setup, we suppose the saddle lies on the boundary of the basin of attraction of  $x_A$ . That is, we will consider starting initially in the basin of attraction of attractor  $x_A$ , and consider the dynamics of switching as escape from the basin of attraction, which we define as a large fluctuation. In the asymptotic limit as the noise intensity goes to zero, the path away from  $x_A$  will pass through the saddle point,  $x_S$ .

When compared to the effective barrier height, we assume the noise is small, and the mean time to switch is much longer than the relaxation time. Thus, the occurrence of switching is expected to be a rare event. Assuming the event lies in the tail of the distribution, the probability of a switching is an exponential distribution, given as

$$\mathcal{P}_x[x] \propto \exp(-R/D), \quad R = \min \mathcal{R}[x, \eta, \lambda], \quad (3)$$

where

$$\mathcal{R}[x, \eta, \lambda] = \mathcal{R}_\eta[\eta(t)] + \int_{-\infty}^{\infty} \lambda(t) \left[ \dot{x}(t) - f \left( x, \int_0^{\infty} g(\sigma) x(t - \sigma) d\sigma \right) - \eta(t) \right] dt, \quad (4)$$

where  $\lambda(t)$  is a time-dependent Lagrange multiplier. Note that the noise source  $\eta(t)$  may be from any continuous or discrete distribution. Here we assume uncorrelated Gaussian noise defined in equation (2) so that we substitute it into equation (4) as

$$\mathcal{R}_\eta[\eta(t)] = \frac{1}{4} \int \eta^2(t) dt. \quad (5)$$

The main goal to determine the probability of switching is to compute the exponent  $R$ , which, for reasons that will be made clear below, we define as the action, similar to the action in classical mechanics.

### A. The Variational Equations of Motion

To simplify the analysis, we define the following convolution:

$$(g \circledast x)(t) \equiv \int_0^\infty g(\sigma)x(t-\sigma)d\sigma. \quad (6)$$

In order to find the exponent  $\mathcal{R}$  in equations (4) and (5), we look for equations that describe the maximum probability of reaching the state  $x_S$  from the initial state  $x_A$ . The variation  $(\delta\mathcal{R})$  is obtained by varying deviations from the path that minimize  $\mathcal{R}$ . Variation with respect to noise  $\eta(t)$  is  $\eta(t) = 2\lambda(t)$ .

The variation with respect to the Lagrange multiplier  $\lambda(t)$  has the form

$$\dot{x}(t) = f(x(t), (g \circledast x)(t)) + 2\lambda(t).$$

Finally, we look at the variation with respect to  $x$ , which is given by

$$\begin{aligned} \frac{\delta\mathcal{R}}{\delta x} &= \mathcal{R}[x + \mu, \eta, \lambda] - \mathcal{R}[x, \eta, \lambda] \\ &= \int_{-\infty}^\infty \lambda(t) [\dot{\mu}(t) - f(x(t) + \mu(t), (g \circledast x)(t) + (g \circledast \mu)(t)) \\ &\quad + f(x(t), (g \circledast x)(t))] dt. \end{aligned}$$

Taylor expanding the last expression gives

$$\begin{aligned} \frac{\delta\mathcal{R}}{\delta x} &= \int_{-\infty}^\infty \lambda(t) \int_0^\infty g(\sigma) [\dot{\mu}(t) - \mu(t)f_1(x(t), (g \circledast x)(t)) \\ &\quad - f_2(x(t), (g \circledast x)(t))\mu(t-\sigma)] d\sigma dt + \mathcal{O}(\mu^2), \end{aligned} \quad (7)$$

where  $f_i(\cdot, \cdot)$ ,  $i = 1, 2$  are

$$f_1 = \frac{\partial f(x(t), (g \circledast x)(t))}{\partial x} \quad \text{and} \quad f_2 = \frac{\partial f(x(t), (g \circledast x)(t))}{\partial (g \circledast x)(t)}.$$

Evaluating the second integral in (7) gives the equation of motion for  $\lambda$  in the form:

$$\begin{aligned} -\dot{\lambda}(t) &= \lambda(t)f_1(x(t), (g \circledast x)(t)) \\ &\quad + \int_0^\infty \lambda(t+\sigma)g(\sigma)f_2[x(t+\sigma), (g \circledast x)(t+\sigma)] d\sigma. \end{aligned} \quad (8)$$

Note that unlike the equations for the noise and the state functions, the last equation contains both delayed and advanced terms, making it an acausal equation of motion for  $\lambda(t)$ . Combining the derived variational results leads to a system of equations in the form

$$\dot{x}(t) = f(x, (g \otimes x)(t)) + 2\lambda(t), \quad (9)$$

$$\begin{aligned} \dot{\lambda}(t) = & -\lambda(t)f_1(x(t), (g \otimes x)(t)) \\ & - \int_0^\infty \lambda(t+\sigma)g(\sigma)f_2[x(t+\sigma), (g \otimes x)(t+\sigma)]d\sigma, \end{aligned} \quad (10)$$

which has the Hamiltonian

$$H(x, (g \otimes x)(t), \lambda) = \lambda^2 + \lambda f(x(t), (g \otimes x)(t)). \quad (11)$$

## B. Boundary conditions

To solve for the most likely, or optimal, path along which the system switches from the attractor, we assume we start at or near  $x_A$ , and compute the path to the saddle point  $x_S$  using the equation (10). In order to compute the actual path, boundary conditions are required on the real line. We assume that at steady state, the noise goes to zero. Therefore, we have that as  $t \rightarrow \infty$ ,  $(x(t), \lambda(t)) \rightarrow (x_S, 0)$ . On the other hand, as  $t \rightarrow -\infty$ , we have  $(x(t), \lambda(t)) \rightarrow (x_A, 0)$ .

When noise  $\eta(t) \equiv 0$ , we can linearize the equation (1) about a steady state,  $\bar{x}$ :

$$\dot{X}(t) = f_1(\bar{x}, \bar{x})X(t) + f_2(\bar{x}, \bar{x})(g \otimes X)(t). \quad (12)$$

In particular, when  $\bar{x} = x_A$ , the spectrum of the characteristic equation has values in the left half of the complex plane. In contrast, when  $\bar{x} = x_S$ , at least one eigenvalue has positive real part.

On the other hand, since the equation (8) is linear in  $\lambda$ , at the steady state  $\bar{x}$  we have

$$\dot{\Lambda}(t) = -\Lambda(t)f_1(\bar{x}, \bar{x}) - f_2(\bar{x}, \bar{x}) \int_0^\infty g(\sigma)\Lambda(t+\sigma)d\sigma. \quad (13)$$

Assuming  $\Lambda(t) = e^{\alpha t}$ , the characteristic equation for  $\Lambda$  is,

$$-\alpha - f_1(\bar{x}, \bar{x}) - f_2(\bar{x}, \bar{x})[\{\mathcal{L}g\}(-\alpha)] = 0, \quad (14)$$

where  $\alpha$  is an eigenvalue of a Jacobian, and

$$\{\mathcal{L}g\}(z) = \int_0^\infty e^{-zu}g(u)du,$$

is the Laplace transform of the function  $g(u)$ . Moreover, it is easy to show that the spectrum of  $\Lambda$  have opposite signs to that of  $X$ . Therefore, the attractor becomes a saddle, and saddle remains a saddle. This result will hold true if the mean value of the delay distribution is small.

The interpretation of the local saddle structure and the escape path is such that at attractor  $x_A$ , the conjugate variable supplies an unstable direction for escape through  $x_S$ . Escape occurs along the most probable path which connects saddles  $(x_A, 0)$  to  $(x_S, 0)$  as a heteroclinic orbit. That is, as  $t \rightarrow -\infty$ , the path approaches  $(x_A, 0)$  along its unstable manifold, while as  $t \rightarrow \infty$ , the path asymptotes to  $(x_S, 0)$  along the stable manifold.

### C. Perturbation Theory

Taking into account the above-mentioned assumptions on the equations of motion and asymptotic boundary conditions, the problem of finding the action  $\mathcal{R}$  is formulated as calculating the solutions to a nonlinear two-point boundary problem. We assume that this solution exists in the non-delayed case, and when the delay is non-zero, the corresponding solution remains close to the non-delayed solution. Thus the variational problem of finding the action is formulated as finding its perturbation to non-delayed case. We assume that if  $x(t)$  is a solution for a non-delayed problem, then the perturbations  $\left[ x(t) - \int_0^\infty g(z)x(t-z)dz \right]$  should remain small. The action can be written as the following perturbation problem

$$\mathcal{R}[x, \eta, \lambda] = \mathcal{R}_0[x, \eta, \lambda] + \mathcal{R}_1[x, \eta, \lambda],$$

where

$$\mathcal{R}_0[x, \eta, \lambda] = \frac{1}{4} \int \eta^2(t) dt + \int \lambda(t) [\dot{x}(t) - f(x, x) - \eta(t)] dt, \quad (15)$$

and

$$\mathcal{R}_1[x, \eta, \lambda] = \int \lambda(t) [f(x(t), x(t)) - f(x(t), (g \otimes x)(t))] dt. \quad (16)$$

The minimizing solution can be found by first analyzing the equations that minimize  $\mathcal{R}_0$ , which are denoted by  $[x_o, \eta_o, \lambda_o]$ , and then evaluating the first order correction at the zeroth order solution; i.e.,  $\mathcal{R}_1[x_o, \eta_o, \lambda_o]$ .

From equations (15) and (16), it is easy to see that the optimal path for the non-delayed case is given by  $\lambda_0 = -f(x_0, x_0)$ , implying that  $\dot{x}_0 = -f(x_0, x_0)$ , which is just



a time-reversed trajectory from the zero delay case. The optimal noise is then given by  $\eta_0(t) = 2\lambda_0(t)$ .

In order to make further analytical progress, we need to specify a particular choice of the distribution kernel  $g(u)$  and of the function  $f(\cdot)$ . In this paper we consider two particular distributions, namely, a uniform and a two-peak distribution kernel, and a quadratic nonlinearity in the function  $f(\cdot)$ .

### III. UNIFORMLY DISTRIBUTED DELAY

In this section we consider the case of the uniformly distributed kernel that can be written as follows,

$$g(u) = \begin{cases} \frac{1}{2\rho}, & \tau - \rho \leq u \leq \tau + \rho, \\ 0, & \text{otherwise.} \end{cases} \quad (17)$$

With this distribution kernel, we choose the function  $f(\cdot)$  to be

$$f(x(t), (g \otimes x)(t)) = x(1 - x) - \frac{\gamma}{2\rho} \int_{\tau-\rho}^{\tau+\rho} x(t - z) dz. \quad (18)$$

Substituting the expression (18) into the right-hand side of the equation (1), one obtains

$$\dot{x}(t) = x(1 - x) - \frac{\gamma}{2\rho} \int_{\tau-\rho}^{\tau+\rho} x(t - z) dz + \eta(t). \quad (19)$$

#### A. Steady State Stability

In the absence of noise, the equation (19) has two steady states,

$$x_A = 1 - \gamma \quad \text{and} \quad x_S = 0, \quad 0 \leq \gamma \leq 1.$$

To study the stability of these steady states, we substitute the Laplace transform of the distribution kernel

$$\{\mathcal{L}g\}(-\alpha) = \frac{1}{2\rho\alpha} e^{\alpha\tau} (e^{\alpha\rho} - e^{-\alpha\rho}) = e^{\alpha\tau} \frac{\sinh(\alpha\rho)}{\alpha\rho}.$$

into the characteristic equation (14) for the conjugate variable,  $\Lambda$ . (Note that since the spectra for  $X$  and  $\Lambda$  characteristic equations are of opposite sign, we only examine the one

for  $\Lambda$ .) Using the Taylor expansion for small mean time delays (and hence, for small  $\rho$ ), we can simplify the characteristic equation and find eigenvalues  $\alpha$  as

$$-\alpha - 1 + 2\bar{x} + \gamma(1 + \alpha\tau) = 0 \implies \alpha = \frac{1 - 2\bar{x} - \gamma}{\gamma\tau - 1}.$$

At the steady state  $\bar{x} = x_A$ , we have  $\alpha = \frac{1-\gamma}{1-\gamma\tau} > 0$  for  $\Lambda$ , and  $\alpha = \frac{1-\gamma}{1-\gamma\tau} < 0$  for  $X$ . Similar but opposite sign results hold for  $x_S$ .

Therefore, when  $t \rightarrow -\infty$ , the solution of the linearized problem tends to  $(x_A, 0)$ , and the solution of the linearized problem tends to  $(x_S, 0)$  as  $t \rightarrow \infty$ .

## B. Perturbation of the Action

In order to find the optimal path from  $x_A$  to  $x_S$ , which minimizes  $\mathcal{R}_0$ , we use the fact that the optimal path solutions satisfy  $\dot{x}_o(t) = -f(x_o(t), x_o(t))$  and  $\lambda_o = -f(x_o(t), x_o(t))$ .

For the vector field without delay, we find that

$$x_o = \frac{x_A}{1 + e^{x_A t}}, \quad (20)$$

that as  $t \rightarrow \infty$ ,  $x_o(t) \rightarrow 0$ , and as  $t \rightarrow -\infty$ ,  $x_o(t) \rightarrow x_A$  and

$$\mathcal{R}_0(\tau, \rho) = \frac{x_A^3}{3}. \quad (21)$$

Since

$$f(x(t), x(t)) - f(x(t), (g \otimes x)(t)) = -\gamma \left[ x(t) - \frac{1}{2\rho} \int_{\tau-\rho}^{\tau+\rho} x(t-z) dz \right],$$

the first order action can be found as

$$\begin{aligned} \mathcal{R}_1(\tau, \rho) &= -2\gamma \int_{-\infty}^{\infty} \dot{x}_o(t) \left[ x_o(t) - \frac{1}{2\rho} \int_{\tau-\rho}^{\tau+\rho} x_o(t-z) dz \right] dt. \\ &= -2\gamma \int_{-\infty}^{\infty} -x_o(x_A - x_o) \left[ x_o(t) - x_A - \frac{1}{2\rho} \ln \left( \frac{1 + e^{x_A(t-\tau-\rho)}}{1 + e^{x_A(t-\tau+\rho)}} \right) \right] dt. \end{aligned} \quad (22)$$

Combining the above calculations, the expression for  $\mathcal{R}(\tau, \rho)$  becomes

$$\mathcal{R}(\tau, \rho) = \frac{x_A^3}{3} - \gamma x_A^2 - \frac{\gamma}{\rho} \cdot \frac{x_A^2(\tau + \rho)}{e^{x_A(\tau+\rho)} - 1} + \frac{\gamma}{\rho} \cdot \frac{x_A^2(\tau - \rho)}{e^{x_A(\tau-\rho)} - 1}, \quad (23)$$

where we have an explicit dependence on the mean time delay  $\tau$  and the distribution width

$\rho$ . For small distribution widths  $\rho$ , this expression can be further expanded as

$$\begin{aligned} \mathcal{R}(\tau, \rho) \approx & \frac{x_A^3}{3} - 2\gamma \left( -\frac{x_A^2}{2} + \frac{x_A^2 e^{x_A \tau} (e^{x_A \tau} - x_A \tau - 1)}{(e^{x_A \tau} - 1)^2} \right) \\ & + \frac{1}{3} \frac{x_A^4 e^{x_A \tau} (-3e^{2x_A \tau} + 3 + x_A \tau e^{2x_A \tau} + 4x_A \tau e^{x_A \tau} + x_A \tau)}{(e^{x_A \tau} - 1)^4} \rho^2 + \mathcal{O}(\rho^4). \end{aligned} \quad (24)$$

If  $\rho = 0$ , then we recover the same expression as in [41], which was derived for the case of the discrete time delay.

#### IV. A TWO-PEAK DELAY DISTRIBUTION KERNEL

In this section we analyze the effect of distributed delay on the switching rates by considering a distribution kernel  $g(u)$  in the form of two discrete time delays with an average delay  $\tau$ , which are separated by a time interval  $2\rho$  [51]. Under this approximation, the distribution kernel  $g(u)$  can be written as

$$g(u) = \frac{\delta(u - \tau - \rho) + \delta(u - \tau + \rho)}{2},$$

where  $\delta$  is the Dirac delta function. For simplicity, we introduce the notation as follows

$$\tau + \rho = \tau_1, \quad \tau - \rho = \tau_2,$$

and

$$x_{\tau_1} = x(t - \tau_1), \quad x_{\tau_2} = x(t - \tau_2).$$

The calculations for the variation with respect to noise and  $\lambda(t)$  will be similar to those in Section II, so we just state the one variation with respect to  $x(t)$ , since the problem now involves multiple delays. Looking at the deviation with respect to  $x(t)$  gives:

$$\begin{aligned} \frac{\delta \mathcal{R}}{\delta x} = & - \int \mu(t) \left[ \dot{\lambda}(t) + \lambda(t) \frac{\delta f(x, x(t - \tau_1), x(t - \tau_2))}{\delta x(t)} \right. \\ & - \lambda(t + \tau_1) \frac{\delta f(x(t + \tau_1), x(t), x(t + 2\rho))}{\delta x(t - \tau_1)} \\ & \left. - \lambda(t + \tau_2) \frac{\delta f(x(t + \tau_2), x(t - 2\rho), x(t))}{\delta x(t - \tau_2)} \right] dt. \end{aligned}$$

Now, the equations of motion can be written in the following way

$$\dot{x}(t) = f(x(t), x(t - \tau_1), x(t - \tau_2)) + 2\lambda(t),$$

$$\begin{aligned} \dot{\lambda}(t) = & -\lambda(t) \frac{\delta f(x, x(t - \tau_1), x(t - \tau_2))}{\delta x(t)} \\ & - \lambda(t + \tau_1) \frac{\delta f(x(t + \tau_1), x(t), x(t + 2\rho))}{\delta x(t - \tau_1)} - \lambda(t + \tau_2) \frac{\delta f(x(t + \tau_2), x(t - 2\rho), x(t))}{\delta x(t - \tau_2)}. \end{aligned}$$

We remark that since the problem is one with multiple delays, the equations of motion can be derived using the Hamiltonian:

$$H(x, x_{\tau_1}, x_{\tau_2}, \lambda) = \lambda^2 + \lambda f(x, x_{\tau_1}, x_{\tau_2}),$$

with the general acausal equations of motion:

$$\begin{aligned} \dot{x}_o = & \frac{\partial H}{\partial \lambda}(x_o, x_{o\tau_1}, x_{o\tau_2}, \lambda_o), \\ \dot{\lambda}_o = & -\frac{\partial H}{\partial x}(x_o, x_{o\tau_1}, x_{o\tau_2}, \lambda_o) - \frac{\partial H}{\partial x_{\tau_1}}(x_o(t + \tau_1), x_o(t), x_o(t + 2\rho), \lambda_o(t + \tau_1)) \\ & - \frac{\partial H}{\partial x_{\tau_2}}(x_o(t + \tau_2), x_o(t - 2\rho), x_o(t), \lambda_o(t + \tau_2)). \end{aligned}$$

In order to compute the optimal path, we assume that the solution exists for  $\tau_{1,2} = 0$ , and the solutions for  $\tau_{1,2} \neq 0$  remain close to the non-delayed solution, and as before we assume that perturbations to the optimal path when  $\tau_{1,2} \neq 0$  remain small. This means that if  $x(t)$  is a solution for  $\tau_{1,2} = 0$ , then the perturbations  $\delta x_{\tau_i} \equiv x(t) - x(t - \tau_i)$ ,  $i = 1, 2$ , should remain small. The action is formulated using the perturbation problem given in equations (15) and (16) for  $\mathcal{R}_0[x, \eta, \lambda]$  and  $\mathcal{R}_1[x, \eta, \lambda]$ , where

$$\mathcal{R}_0[x, \eta, \lambda] = \frac{1}{4} \int \eta^2(t) dt + \int \lambda(t) [\dot{x}(t) - f(x, x, x) - \eta(t)] dt,$$

and

$$\mathcal{R}_1[x, \eta, \lambda] = \int \lambda(t) [f(x(t), x(t), x(t)) - f(x(t), x(t - \tau_1), x(t - \tau_2))] dt,$$

so the action now explicitly depends on two constant time delays  $\tau_1$  and  $\tau_2$ . In order to compare the results of the two-peak distribution kernel with the results on uniform distribution obtained in Section III, as well as to the case of the single discrete time delay considered in [41], we consider function  $f$  as follows,

$$f(x, x_{\tau_1}, x_{\tau_2}) = x(1 - x) - \frac{\gamma}{2}(x_{\tau_1} + x_{\tau_2}).$$

When  $\eta(t) = 0$ , there are two steady states

$$x_A = 1 - \gamma \quad \text{and} \quad x_S = 0, \quad 0 \leq \gamma \leq 1.$$

Linearizing near the steady states, using the characteristic equation (14), yields

$$-\alpha - 1 + 2\bar{x} + \frac{\gamma}{2}(1 + \alpha\tau_1 + 1 + \alpha\tau_2) = 0 \quad \implies \quad \alpha = \frac{1 - 2\bar{x} - \gamma}{(\gamma/2)(\tau_1 + \tau_2) - 1} = \frac{1 - 2\bar{x} - \gamma}{\gamma\tau - 1},$$

and the stability characteristics of the attractor and saddle are exactly the same as in the previous section.

In the absence of delay, the computation of  $\mathcal{R}_0$  is the same as before, and we only need to compute  $\mathcal{R}_1$ . Since

$$f(x, x, x) - f(x, x_{\tau_1}, x_{\tau_2}) = -\frac{\gamma}{2}[(x - x_{\tau_1}) + (x - x_{\tau_2})],$$

we can find the first order action as

$$\begin{aligned} \mathcal{R}_1(\tau_1, \tau_2) &= -\gamma \int_{-\infty}^{\infty} \dot{x}_o(t)[x_o(t) - x_o(t - \tau_1)]dt - \gamma \int_{-\infty}^{\infty} \dot{x}_o(t)[x_o(t) - x_o(t - \tau_2)]dt. \\ &= 2\gamma \int_{-\infty}^{\infty} \frac{x_A^3}{(1 + e^{x_A t})^3} dt - \gamma x_A^3 \int_{-\infty}^{\infty} \frac{e^{x_A t}}{(1 + e^{x_A t})^2(1 + e^{x_A(t-\tau_1)})} dt \\ &\quad - \gamma x_A^3 \int_{-\infty}^{\infty} \frac{e^{x_A t}}{(1 + e^{x_A t})^2(1 + e^{x_A(t-\tau_2)})} dt. \end{aligned}$$

Evaluating the integrals in the last expression gives the first order action  $\mathcal{R}_1(\tau_1, \tau_2)$  and the full action to the first order in  $\delta x(t)$  can be found as

$$\mathcal{R}(\tau_1, \tau_2) \approx \frac{x_A^3}{3} - \gamma x_A^2 \left( -1 + \frac{e^{x_A \tau_1}[-x_A \tau_1 - 1 + e^{x_A \tau_1}]}{(e^{x_A \tau_1} - 1)^2} + \frac{e^{x_A \tau_2}[-x_A \tau_2 - 1 + e^{x_A \tau_2}]}{(e^{x_A \tau_2} - 1)^2} \right), \quad (25)$$

where  $\tau_1 = \tau + \rho$  and  $\tau_2 = \tau - \rho$ . If the width  $\rho = 0$ , the time delays  $\tau_1$  and  $\tau_2$  coincide, and the expression (25) becomes the same as the one derived in [41] for the case of the single time delay.

## V. NUMERICAL SIMULATIONS

In this section we perform numerical simulations of the system (1) with uniform and two-peak distribution kernels, given by (19) in order to compare theoretical predictions for switching times. Following the same methodology as in [41], we calculate the mean switching times  $T_{st}$  as the noise  $\eta(t)$  takes the system out of the basin of attraction of the steady state

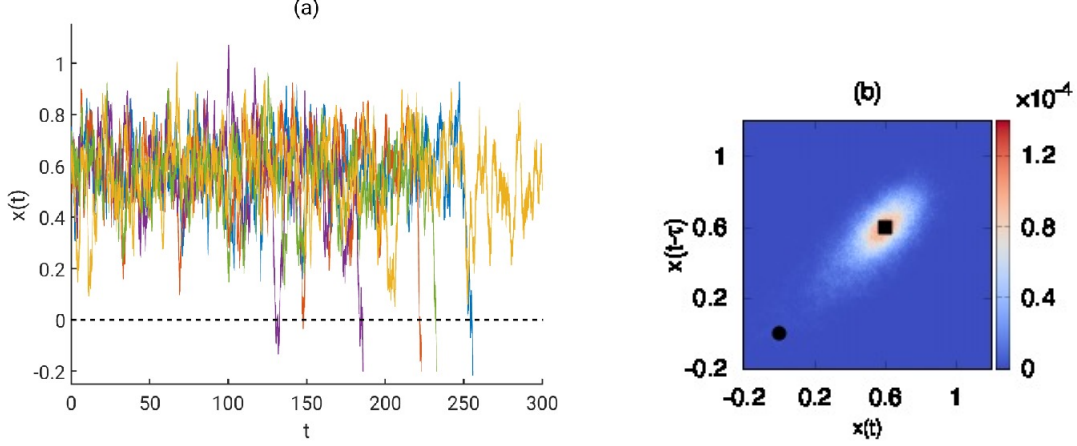


FIG. 1. (a) Sample switching time series in (19) and (b) a probability density of switching obtained by numerical simulations for the uniformly distributed kernel. Black squares (circles) denote the attractor (saddle point). Parameters are:  $\gamma = 0.4$ ,  $\sqrt{2D} = 0.12$ ,  $\tau = 0.8$ ,  $\rho = 0.5$ .

$x_A$  to  $x < x_S$ . Numerical simulations are run for some time after the trajectory passes  $x_S$  to ensure that the probability of its return to the basin of attraction of the stable steady state  $x_A$  is exponentially small. Numerical simulations are performed using the Heun or stochastic predictor-corrector method [52, 53], in which the solution to equation (1) is approximated using the following iterative scheme

$$x_{n+1} = x_n + \frac{1}{2}(K_n + K_{n+1})h + \sqrt{2D}hu,$$

with a step size  $h$ ,  $u$  is  $\mathcal{N}(0, 1)$ , and

$$K_n = x_n(1 - x_n) - Y_n, \quad K_{n+1} = \bar{x}_{n+1}(1 - \bar{x}_{n+1}) - Y_{n+1},$$

where the approximation to  $\bar{x}_{n+1}$  is given by

$$\bar{x}_{n+1} \approx x_n + K_n h + \sqrt{2D}hu.$$

The terms  $Y_n$  and  $Y_{n+1}$  representing the delay distribution were computed using a composite trapezoidal rule in the case of uniform distribution, and for the two-peak distribution these were given by

$$Y_n = \frac{1}{2}(x_{n-k_1} + x_{n-k_2}), \quad Y_{n+1} = \frac{1}{2}(x_{n+1-k_1} + x_{n+1-k_2}),$$

where  $k_1 h = \tau - \rho$  and  $k_2 h = \tau + \rho$ .

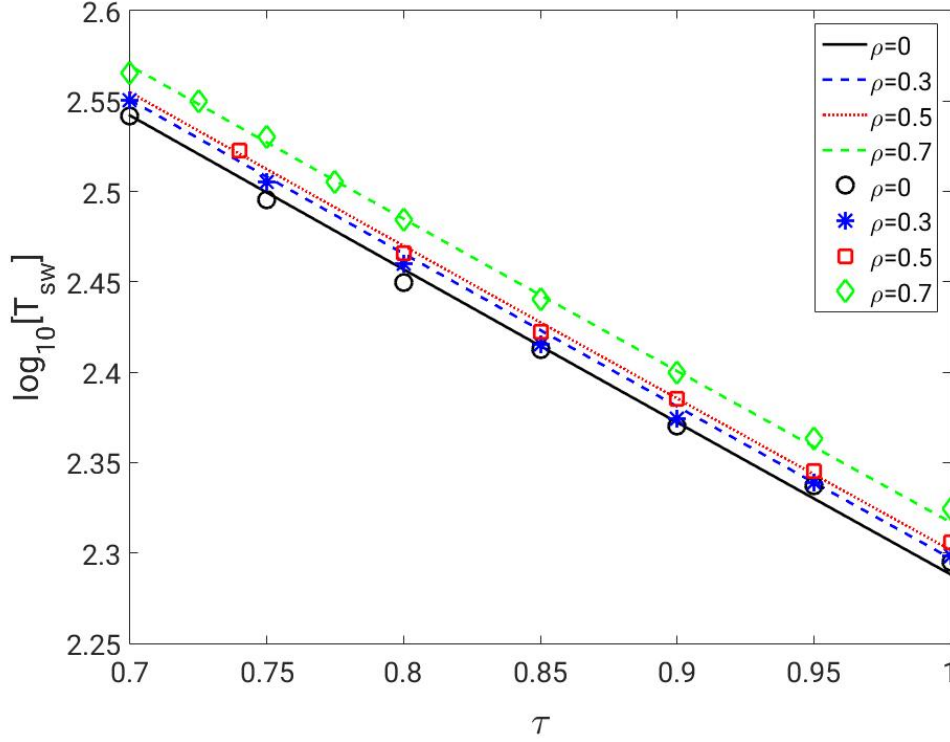


FIG. 2. A comparison of the first order perturbation theory in time delay  $\tau$  given by (19) and the  $\log_{10}$  of the mean switching times obtained by numerical simulations for the uniformly distributed kernel for several values of the distribution width  $\rho$ . Solid lines are theoretical predictions, and symbols are numerical simulations. Other parameters are:  $\gamma = 0.4$ ,  $\sqrt{2D} = 0.12$ ,  $\tau = 0.8$ .

Examples of switching time series for several runs are shown in Figs. 1(a) and 3(a) for the uniform and bi-modal delay distributions, respectively. One can see that the dynamics fluctuates around a mean value of the attractor for long period of time until at some point there is a large change in which the dynamics passes through the saddle at the origin. The accompanying probability densities in panel (b) illustrate the fact that most of the time the dynamics are in the neighborhood of the attractor. Although the probability density plots show many paths to going from  $x_A$  to the saddle at the origin, they also contain the most probable path to switch.

The switching rate is proportional to the probability of large fluctuations  $\mathcal{P}_x[x]$  introduced in Section II, and the switching time is the inverse of the switching rate. Using the equation (3), the switching time can be found as

$$T_{sw} = c_{sw} \exp(R_{sw}/D),$$

where  $R_{sw}$  is given by the approximation (24) for the uniformly distributed delay kernel, and the expression (25) in the case of the two delay kernel approximation. Since the noise is Gaussian, the constant  $c_{sw}$  can be found using the Kramer's theory [54] at zero delay. This constant for non-zero delay corresponds to the approximate vertical shift of the theoretical results when  $T_{sw}$  is plotted on the logarithmic scale, and is assumed to have weak dependence on noise and delay.

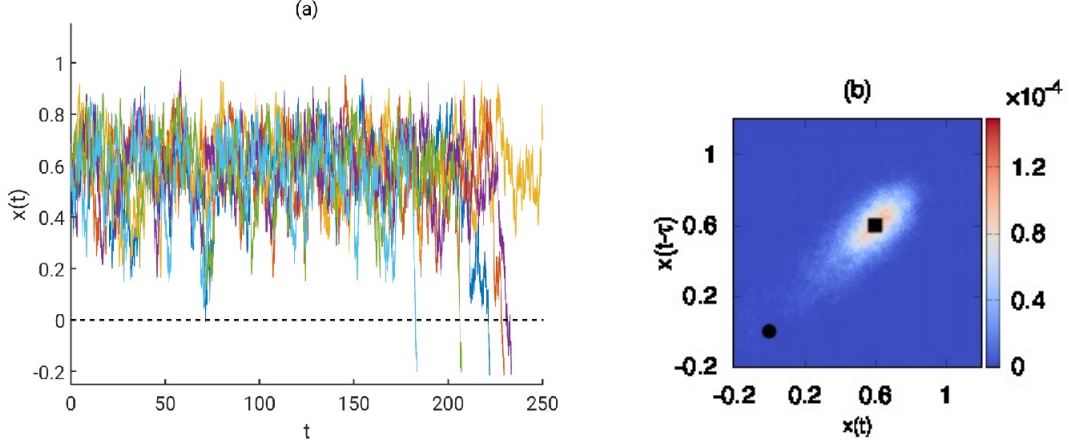


FIG. 3. a) Sample switching time series in two-peak delay distribution and (b) a probability density of switching obtained by numerical simulations. Black squares (circles) denote the attractor (saddle point). Parameters are:  $\gamma = 0.4$ ,  $\sqrt{2D} = 0.12$ ,  $\tau = 0.8$ ,  $\rho = 0.5$ .

In Figs. 2 and 4, the lines represent theoretical approximations as the first order in  $\tau$  perturbation theory given by the expressions (24) and (25), and circles are the mean values of the numerical simulations taken over 2000 simulations. In Fig 2, we show the comparison between the theoretical results and numerical simulations of the switching time as the function of mean time delay  $\tau$  for the case of uniformly distributed kernel for several values of the distribution width  $\rho$ . It can be seen that increasing the mean time delay  $\tau$  for any distribution width  $\rho$  leads to the decrease in the switching times  $T_{sw}$ , and theoretical predictions align well with numerical simulations all the way up to  $\tau = 1$ . It is also clear that increasing the distribution width leads to the increase in the switching times even for small values of the mean time delay  $\tau$ , and this increase in switching times is maintained for a whole range of admissible values of  $\tau$  ( $\tau < \rho$ ).

A similar situation is observed in Fig 4, which shows the comparison between theory and numerical simulations for the case of the two-peak distributed kernel, given by two discrete



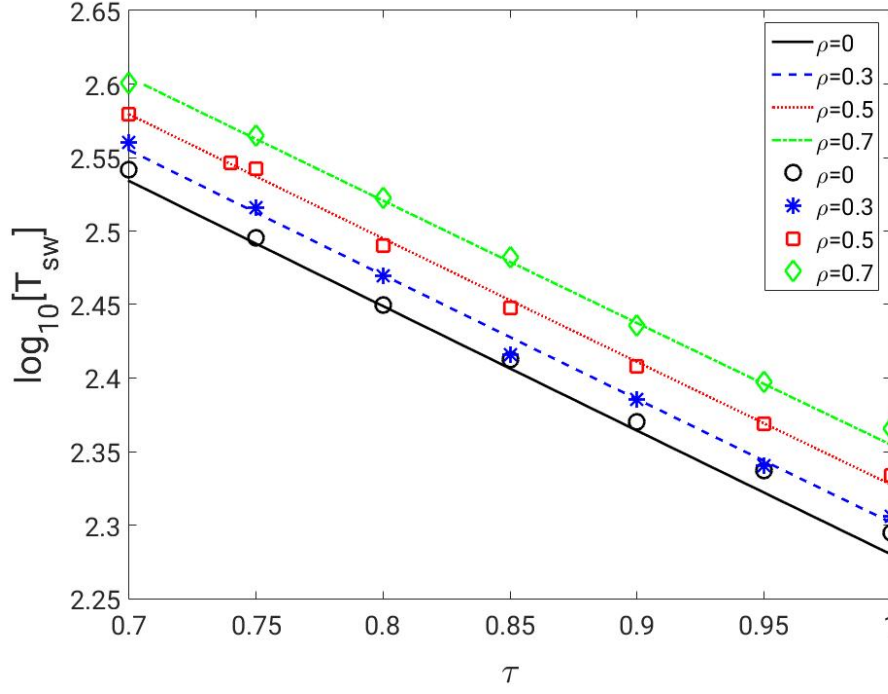


FIG. 4. A comparison of the first order perturbation theory in time delay  $\tau$  and the  $\log_{10}$  of the mean switching times obtained by numerical simulations for two-peak distribution kernel for several values of the distribution width  $\rho$ . Solid lines are theoretical predictions, and symbols are numerical simulations. Other parameters are:  $\gamma = 0.4$ ,  $\sqrt{2D} = 0.12$ ,  $\tau = 0.8$ .

time delays separated by a time interval of  $2\rho$ . Again, analytical results and numerical simulations are in an excellent agreement for mean time delays up to  $\tau = 1$ . The fastest switching times are achieved when the width  $\rho$  is equal to zero, corresponding to the case of a single discrete time delay in model (1), and when the mean time delay  $\tau$  is large enough. As the distribution width  $\rho$  becomes larger, the switching time for the trajectory to be pushed out of the basin of attraction of the steady state increases over the whole range of time delays  $\tau$ . This clearly shows that in delayed systems, not only the value of the mean time delay plays a role in determining the escape rates/times, but the width of the distribution also has an important influence on the overall dynamics, and the escape rates in particular. Moreover, comparing Figs. 2 and 4, it is worth noting, that while in both cases the switching times grow for larger distribution widths, the growth is more pronounced in the case of the two-peak distribution.

## VI. DISCUSSION

In this paper we have considered the problem of finding escape rates from the basin of attraction of the stable steady state in a dynamical system with distributed time delays and Gaussian noise. In the absence of noise, the system has stable and unstable steady states, and the solutions initially in the basin of attraction of the stable steady state remain in the basin. When the noise is included, most of the time the solution trajectories will fluctuate around the stable steady state. However, there exist rare instances where noise acts as a coherent force, resulting in a trajectory that takes the system out of the attractor's basin of attraction. Here we have aimed to understand how particular delay distributions influence the escape rates/times as compared to a single discrete time delay situation. In order to calculate the escape rate, the problem has been formulated for a general distribution kernel as a variational problem along the optimal path, which maximizes the probability of escape. Since noise-induced switching occurrences are rare events, the optimal solution to the variational problem is valid in the tail of the distribution, which is exponential. We also note that even small changes in the action lead to exponential changes in switching probability and switching times.

In order to make further analytical progress, having obtained the variational equations for the extreme trajectories for a general distribution, we have then considered two particular cases of the distribution kernel, namely, uniform and two time delay (two-peak) distributions. For both of those distributions, we have been able to obtain closed form analytical expressions for the escape rates, which explicitly depend on the mean delay and distribution width. The exemplified results hold near a trans-critical bifurcation point. It is known that the exponent of the probability of escape from the attractor scales linearly with distance from the bifurcation point when the delay is zero. In contrast, we note that the scaling exponent of a saddle-node bifurcation scales as  $\chi^{3/2}$ , where  $\chi$  is the distance to the bifurcation point. [41]

We have performed numerical simulations for both distribution kernels and compared the results of the theoretical predictions for the escape time to the numerically calculated ones. We have found very good agreement between theoretical prediction based on the small-delay approximation, and numerical simulations for mean time delay values up to  $\tau = 1$ . We have also compared theoretical and numerical results for larger values of time delay  $\tau$ , but found

that they start to diverge for larger time delays, suggesting that the linear approximation does not work well for large time delays.

We have found that the fastest switching times for all values of the time delay are in the case when the distribution width is equal to zero for both examples of the distribution kernel considered. As the distribution width is increased, the switching times are decreasing even for the large values of the mean time delay. Moreover, comparing the change in switching times for uniform and two-peak distribution, we have found that while both do increase escape times, the latter has a more profound effect. This strongly indicates that not only the mean time delay plays a role in the switching dynamics, but the width and the choice of the distribution are another two important factors that influence exponentially the switching rates in time-delayed systems.

In this paper we have concentrated on the influence of the delay distribution on the switching rates in the presence of Gaussian noise and have used two particular distribution kernels. The next step would be to analyze the influence of the Gamma distributed kernel (for weak and strong Gamma kernels) and compare the results to the cases of a single discrete time delay studied in [41], and of the uniform and two-peak distributions considered in this paper. The model studied in this paper has a saddle point and only a single stable steady state. Another important future direction of this research would be to analyze the influence of the delay distribution on the switching times in bistable systems.

## VII. ACKNOWLEDGMENTS

The authors gratefully acknowledge support from the Office of Naval Research under contract numbers N0001418WX01225 and N0001412WX20083, and support of the NRL Base Research Program N0001412WX30002.

- 
- [1] T. Erneux, Applied delay differential equations (Springer, Springer, New York, 2009).
  - [2] J. Bélair, S. A. Campbell, and P. van den Driessche, SIAM J. Appl. Math. **56**, 245 (1996).
  - [3] R. Rahman, K. Blyuss, and Y. Kyrychko, SIAM J. Appl. Dyn. Sys. **14**, 2069 (2015).
  - [4] T. Heil, I. Fischer, W. Elsässer, J. Mulet, and C. Mirasso, Phys. Rev. Lett. **86**, 795 (2001).
  - [5] H. Pichler and P. Zoller, Phys. Rev. Lett. **116**, 093601 (2016).

- [6] S. M. Hein, F. Schulze, A. Carmele, and A. Knorr, *Phys. Rev. A* **91**, 052321 (2015).
- [7] S.-L. Wu, P. Weng, and S. Ruan, *Europ. J. Appl. Math.* **26**, 61 (2015).
- [8] S. Gourley, J.-H. So, and J. Wu, *J. of Math. Sci.* **142**, 5119 (2004).
- [9] Y. Kyrychko, S. A. Gourley, and M. V. Bartuccelli, *SIAM J. Math. Anal.* **37**, 1688 (2006).
- [10] X. Zhong, S. Guo, and M. Peng, *Stochastic Anal. Appl.* **35**, 1 (2017).
- [11] L. Bauer, J. Bassett, P. Hövel, Y. N. Kyrychko, and K. B. Blyuss, *Chaos: An Interdisciplinary Journal of Nonlinear Science* **27**, 114317 (2017).
- [12] C. Gupta, J. M. López, R. Azencott, M. R. Bennett, K. Josić, and W. Ott, *J. Chem. Phys.* **140**, 204108 (2014).
- [13] K. Parmar, K. Blyuss, Y. Kyrychko, and S. Hogan, *Comp. and Math. Methods in Medicine* **2015**, 347273 (2015).
- [14] J. Feng, S. A. Sevier, B. Huang, D. Jia, and H. Levine, *Phys. Rev. E* **94**, 032408 (2016).
- [15] K. Szwaykowska, I. B. Schwartz, L. Mier-y Teran Romero, C. R. Heckman, D. Mox, and M. A. Hsieh, *Phys. Rev. E* **93**, 032307 (2016).
- [16] J. Hindes, K. Szwaykowska, and I. B. Schwartz, *Phys. Rev. E* **94**, 032306 (2016).
- [17] G. Burgers, *Climate Dynamics* **15**, 521 (1999).
- [18] C. Ping, L. Ji, H. Li, and M. Flügel, *Physica D* **98**, 301 (1996).
- [19] A. Keane, B. Krauskopf, and C. Postlethwaite, *SIAM J. Appl. Dyn. Sys.* **14**, 1229 (2015).
- [20] A. Zakharova, N. Semenova, V. Anishchenko, and E. Schöll, *Chaos* **27**, 114320 (2017).
- [21] T. Frank, *Phys. Lett. A* **357**, 275 (2006).
- [22] T. Frank, *Phys. Lett. A* **380**, 1341 (2016).
- [23] P. Ashwin, S. Wieczorek, R. Vitolo, and P. Cox, *Phil. Trans. R. Soc. A* **370**, 1166 (2012).
- [24] T. Nishikawa and E. Ott, *Chaos* **24**, 033107 (2014).
- [25] P. Ritchie and J. Sieber, *Chaos* **26**, 093116 (2016).
- [26] M. I. Freidlin and A. D. Wentzell, Random Perturbations of Dynamical Systems, 2nd ed. (Springer-Verlag, New York, 1998) p. 430.
- [27] A. D. Ventcel', *Teor. Verojatnost. i Primenen.* **21**, 235 (1976).
- [28] R. Graham and T. Tél, *Phys. Rev. Lett.* **52**, 9 (1984).
- [29] R. Graham and F. Moss, *Theory of Continuous Fokker–Planck Systems* **1**, 225 (1989).
- [30] M. I. Dykman and M. A. Krivoglaz, *Physica A* **104**, 480 (1980).
- [31] M. I. Dykman, M. M. Millonas, and V. N. Smelyanskiy, *Phys. Lett. A* **195**, 53 (1994).

- [32] M. I. Dykman, I. B. Schwartz, and A. S. Landsman, Phys. Rev. Lett. **101**, 078101 (2008).
- [33] H. R. Jauslin, Physica A **144**, 179 (1987).
- [34] R. S. Maier and D. L. Stein, Phys. Rev. Lett. **71**, 1783 (1993).
- [35] R. S. Maier and D. L. Stein, SIAM J. Appl. Math. **57**, 752 (1997).
- [36] H. Touchette, Phys. Rep. **478**, 1 (2009).
- [37] A. Kamenev, Field theory of non-equilibrium systems (Cambridge University Press, 2011).
- [38] L. S. Tsimring and A. Pikovsky, Phys. Rev. Lett. **87**, 250602 (2001).
- [39] C. Masoller, Phys. Rev. Lett. **90**, 020601 (2003).
- [40] B. Lindley, L. Mier-y Teran-Romero, and I. B. Schwartz, in American Control Conference (ACC), 2013 (IEEE, 2013) pp. 4587–4591.
- [41] I. B. Schwartz, L. Billings, T. W. Carr, and M. I. Dykman, Phys. Rev. E **91**, 012139 (2015).
- [42] Y. N. Kyrychko, K. B. Blyuss, and E. Schöll, Eur. Phys. J. B Condens. Matter Phys. **14**, 307 (2011).
- [43] Y. N. Kyrychko, K. B. Blyuss, and E. Schöll, Phil. Trans. R. Soc. A **371**, 20120466 (2013).
- [44] Y. N. Kyrychko, K. B. Blyuss, and E. Schöll, Chaos **24**, 043117 (2014).
- [45] R. Sipahi, F. Atay, and S.-I. Niculescu, SIAM J. Appl. Math. **68**, 738 (2008).
- [46] A. Campbell and R. Jessop, Math. Model. Nat. Phenom. **4**, 1 (2009).
- [47] K. Blyuss and Y. Kyrychko, Bull. Math. Biol. **72**, 490 (2010).
- [48] T. Faria and S. Trofimchuk, Nonlinearity **23**, 2457 (2010).
- [49] S. Gourley and J.-H. So, Proc. R. Soc. Edinb. **133**, 527 (2003).
- [50] R. P. Feynman and A. R. Hibbs, Quantum Mechanics and Path Integrals (McGraw–Hill, 1965).
- [51] C. W. Eurich, A. Thiel, and L. Fahse, Phys. Rev. Lett. **94**, 158104 (2005).
- [52] P. Klöden and E. Platen, Numerical solutions of stochastic differential equations (Springer, New York, 1992).
- [53] S. Iacus, Simulation and Inference for Stochastic Differential Equations (Springer, New York, 2008).
- [54] B. Abdo, E. Segev, O. Shtempluck, and E. Buks, J. Appl. Phys. **101**, 083909 (2007).